Orientational order of single-wall carbon nanotubes in stretch-aligned photoluminescent composite films

Camilo Zamora-Ledezma
Laboratorio de Física de la Materia Condensada, Centro de Física, Instituto Venezolano de Investigaciones Científicas, Altos de Pipe, 1024 Caracas, Venezuela
and Laboratoire des Colloïdes, Verres et Nanomatériaux, Université Montpellier II et CNRS, Place Eugène Bataillon, 34090 Montpellier, France

Christophe Blanc and Eric Anglaret*
Laboratoire des Colloïdes, Verres et Nanomatériaux, Université Montpellier II et CNRS, Place Eugène Bataillon, 34090 Montpellier, France

(Received 16 May 2009; revised manuscript received 25 August 2009; published 28 September 2009)

We study the alignment of single-wall carbon nanotubes in polyvinylalcohol composites using polarized Raman and photoluminescence spectroscopies. Nanotubes are well dispersed down to the individual scale in the composites as revealed by the strong photoluminescence signal. Alignment can be continuously adjusted by hot stretching the composites. We propose a simple relation to measure the order parameter based on the assumption that only one single component of the Raman polarizability tensor is nonzero. The similar profiles of spectra measured in different polarization configurations validate this assumption. The orientation of the nanotubes under uniaxial stretching is well modelized by a simple affine model assuming deformation at constant volume.

DOI: 10.1103/PhysRevB.80.113407 PACS number(s): 61.30.Gd, 61.48.−c, 78.55.−m

Composite materials appear very promising for exploiting the remarkable properties of individual carbon nanotubes (CNT) at a macroscopic scale. Functional materials are usually obtained by processing a mixture of CNT and polymers into bulk composites, films, or fibers.[1–4] Their properties are expected to be drastically influenced by the alignment of the nanotubes. For example, the flow alignment of CNT in "super tough" nanotubes-fibers preparation[4–6] yields a dramatic improvement of the mechanical energy absorption along the fiber axis. For most advanced potential applications, an homogeneous dispersion of CNT (Ref. 7) is also required. For instance, the strong anisotropic optical absorption and photoluminescence of individual single-wall carbon nanotubes (SWCNT) make them excellent candidates in the preparation of anisotropic composites for photonic and optoelectronical applications.[8–10] Photoluminescence is however observed only when the tubes are individualized or at least when no contact between metallic and semiconducting SWCNT exist.[11] Electric,[12] optical, thermal, and mechanical properties are also expected to be very sensitive to both the tubes orientational order and the quality of dispersion.

Alignment is conveniently described with the nematic orientational scalar order parameter S.[13] This parameter is useful to compare the ordering in different samples but also helps to quantify the evolution of anisotropic properties with alignment.[14–16] Some efforts have already been paid to measure S in CNT liquid crystal dispersions or in CNT composites by using birefringence, absorbance, x-ray or Raman scattering.[3,14,15,17–19] Most of the measurements are however based on rough assumptions or on hypotheses on the angular distribution shape. A few works only[19–21] have explored the quantitative validation of such methods. For example, Ahir *et al.*[19] measured from x-ray diffraction the order parameter describing nanotube reorientation in a semisolid rubbery sample and found that the actual order was much weaker than expected from an affine model of uniaxial elongation. It should be noted that among the techniques used, Raman spectroscopy appears to be one of the most powerful tools because Raman signal is intense and all modes are strongly polarized along the tube axis.[18,22] Starting from this fact, we recently proposed a simple and accurate method based on only three Raman measurements to compute S in a SWCNT-based uniaxial system.[23] In this communication we focus on the processing of composites where well-dispersed individualized SWCNT are embedded in polyvinylalcohol (PVA), a hydrosoluble polymer. We study their Raman and photoluminescence spectra and show how the polarization studies can be efficiently used to determine the orientational order parameter. The changes observed under strain are then used to test our spectroscopy method over a broad range of order parameters. We finally discuss the validity of the simple affine model of elongation for determining the order parameter in stretched SWCNT composites.

Raw nanotubes bundles synthesized from carbon monoxide (HipCO method)[24] were exfoliated in water either with an anionic surfactant, sodium dodecyl sulfate (SDS), at a fixed weight ratio SWCNT/SDS=(1/1000) or with denaturated DNA with a weight ratio SWCNT/DNA=(1/2). Both molecules are known to efficiently disperse individual CNT.[4,25] After pulse-tip sonication during 3 h at room temperature, homogeneous aqueous suspensions were obtained without any evidence of aggregation. In order to evidence the effective exfoliation of bundles at the individual SWCNT scale, photoluminescence (PL) measurements were performed. Photoemission is indeed observed only from semiconducting SWCNT either isolated or in bundles of a few nanotubes.[11,26] Figure 1 shows the resulting PL intensity maps as a function of both excitation wavelength (from 710 to 770 nm with 5 nm steps obtained from a tunable Ti:Sa laser) and emission wavelength (1000–1400 nm). Each peak in the maps of Fig. 1 corresponds to an electronic emission E_{11} following an E_{22} excitation from a well-identified semi-

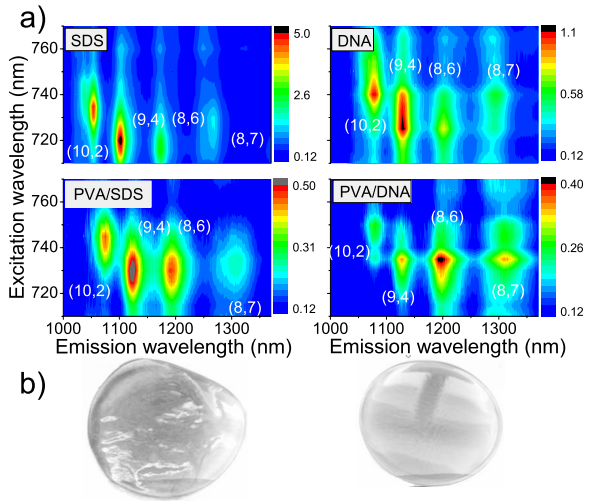

FIG. 1. (Color online) Photoluminescence maps of individualized SWCNT in water suspensions (a, top) stabilized, respectively, with SDS and denaturated DNA. Photoluminescence (a, bottom) is still observed in SWCNT/PVA films [typical films are shown in (b)] obtained from both suspensions. Each peak is assigned to a well-identified nanotube and labeled with its (n,m) integer from Ref. 11. In all maps, each spectrum was corrected for detector sensitivity.

conducting nanotube labeled by its (n,m) integers, where E_{ii} refers to the allowed optical transition between the excitonic states associated with the ith pair of van Hove singularities.[11] Both the position and intensity of each peak change when the surfactant or the matrix change, illustrating the strong environmental dependence of the PL.[11,26–28]

Macroscopic films were obtained by mixing 8 ml of the suspensions with 8 ml of aqueous PVA solution (10 wt. %) in a beaker with a magnetic stirrer during 15 min at room temperature. The resulting homogeneous suspensions were then carefully poured into 9 cm diameter glass Petri dishes. After 48 h of gentle evaporation at room temperature, free standing films of about 100 μm thickness were peeled off. From a SWCNT suspension of concentration 0.01 mg/mL, the resulting films contain 0.01 wt. % of SWCNT. The films prepared with SDS wrinkled during evaporation as shown in Fig. 1 and SWCNT aggregates were observed under microscope. By contrast, films prepared with DNA are flat and homogeneous without any aggregates detected. The PL is redshifted during water evaporation for both type of films. This may be due to the change in the matrix dielectric constant but also to some mechanical strain.[1,8] We also noted that the PL intensity decreases strongly when nanotubes are stabilized with SDS, confirming that part of them aggregate. By contrast, when DNA is used, the PL intensity is nearly constant indicating that the nanotubes remain individualized. The differences in aggregation behavior might be related to the fact that small surfactant molecules are only slightly adsorbed on a nanotube surface[29] whereas long denaturated single strands of DNA strongly cover the tubes surface.[25] It is worth highlighting here that the use of DNA as nanotube coating is not only an efficient way to prepare suspensions of individual SWCNT (Ref. 25) but is also a relevant choice to disperse SWCNT at the individual scale in polymer composites.[2] We will now focus on the elongation of DNA/SWCNT composites and their spectroscopy properties.

Films were fixed on a motorized stretching machine inside an oven to perform hot stretching at 120 °C. At such temperature, above the glass temperature ($T_g \approx 85$ °C) PVA films can be stretched up to 400%. After thermal equilibration, the 5 cm long samples were strained at constant velocity (1.2 cm/min) and then cooled down to room temperature before being removed from the stretching setup. The local strain was accurately measured thanks to a printed grid with initially 1 mm thick marks. We prepared samples with different elongation ratios ($1 \leq \lambda \leq 5$) where λ is the ratio between the length after stretching and the initial length ($\lambda = \varepsilon + 1$ where ε is the elongation strain), and we investigated the local change in both polarized Raman and PL under microscope using a BRUKER RFS100 Fourier transform Raman spectrometer equipped with a laser line excitation source at 1064 nm (1.16 eV) and a nitrogen-cooled germanium detector. As already pointed out,[1,15,18,23] polarized resonant Raman spectroscopy yields quantitative information on the orientation distribution of SWCNT. For a uniaxial sample, the orientation order parameter is defined as a statistical average $S = \langle 3\cos^2\theta - 1\rangle/2$ over the angles θ between the nanotube axis and the stretching axis (corresponding to the director for a nematic liquid crystal). We have shown[23] that S can be calculated from Raman measurements in three different polarization configurations, I_{VV}, I_{HH}, and I_{VH}, where the first and second subscripts, respectively, refer to the polarizations of incident and scattered beams, fixed either parallel (V) or perpendicular (H) to the alignment direction. The method holds provided that (i) the system is uniaxial and (ii) only a single component of the SWCNT Raman polarization tensor is nonzero. Here, the uniaxial stretch supports the first hypothesis. The strong anisotropy of the optical properties of SWCNT and the resonant character of the Raman signal in SWCNT supports that only the zz component of their polarization tensor is nonzero[23] (z is the coordinate along the tube axis). This latter hypothesis was used by several groups to describe the orientational order in anisotropic SWCNT-based systems.[18,30] Note that the second hypothesis also implies that I_{VH}/I_{VV} and I_{HH}/I_{VV} depend only on the angular distribution and that both ratios should decrease to zero for a set of perfectly aligned tubes. On this basis, as derived in Ref. 23, S is given by

$$S = \frac{3I_{VV} + 3I_{VH} - 4I_{HH}}{3I_{VV} + 12I_{VH} + 8I_{HH}}. \quad (1)$$

The evolution of Raman and PL spectra for a laser excitation line at 1064 nm is illustrated in Fig. 2 for three different elongation ratios from weak ($\lambda = 1.4$) to larger strains ($\lambda = 4.2$). The Raman features (narrow peaks in Fig. 2) are typical of SWCNT: radial breathing modes (RBM) are observed at 266 cm^{-1}, tangential modes (TM, also called G band) at 1591 cm^{-1} and the D′ band around 2545 cm^{-1}. In addition, broad PL bands superimpose to the Raman lines (around 1250, 1850, and 2550 cm^{-1} in Fig. 2, corresponding to emission wavelengths of 1225, 1325, and 1400 nm for a laser line at 1064 nm). The observation of the PL bands indicates that nanotubes are individual in the composites. All samples display a maximal intensity when the incident light

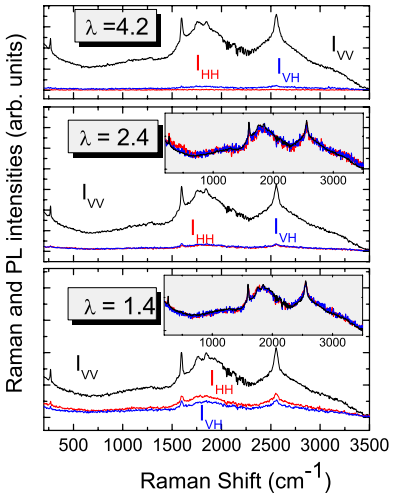

FIG. 2. (Color online) Evolution of Raman and PL spectra of SWCNT/PVA composites excited with a laser line at 1064 nm for different elongation ratios λ. Insets: *VV*, *VH* and *HH* spectra display the same profiles, i.e., the three spectra superimpose after rescaling.

polarization is parallel to the stretching direction. The spectra are highly polarized and both components I_{HH} and I_{VH} decreases rapidly with increasing strains for both Raman and PL signals. At the largest elongation ratio ($\lambda=4.2$), the order parameter is close to 0.8 and the *HH* spectrum vanishes. For all strains, the three spectra (configurations *VV*, *HH*, and *VH*) display the same profiles and can be superimposed over the whole spectral range by a simple normalization as shown in the inserts of Fig. 2. These observations validate the hypothesis that only the *zz* component of the Raman polarizability tensor is at the origin of the Raman signal but also that a similar phenomenon occurs for photoluminescence. They therefore legitimize the use of Eq. (1) and additionally show that S can be accurately determined from the whole spectra rather than from a single Raman peak intensity.

The evolution of the measured order parameter with the elongation ratio is displayed in Fig. 3 and compared to calculated values[19] obtained from a simple affine deformation model of the polymer matrix. In this approach, SWCNT are modeled as inextensible straight cylinders wrapped by polymer envelopes. The initial composites are isotropic, i.e., there is a uniform angular distribution of such cylinders.

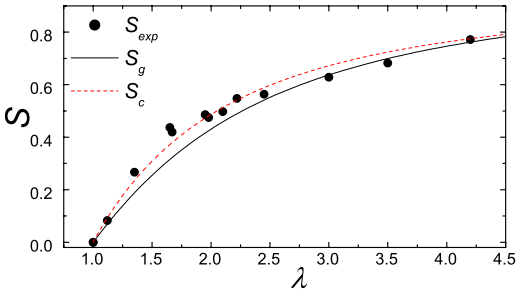

FIG. 3. (Color online) Comparison of the experimental orientational order parameter (dots) to the geometric affine deformation model S_g (solid line) and to the corrected model S_c (dashed line). Size of dots indicates approximate error bars.

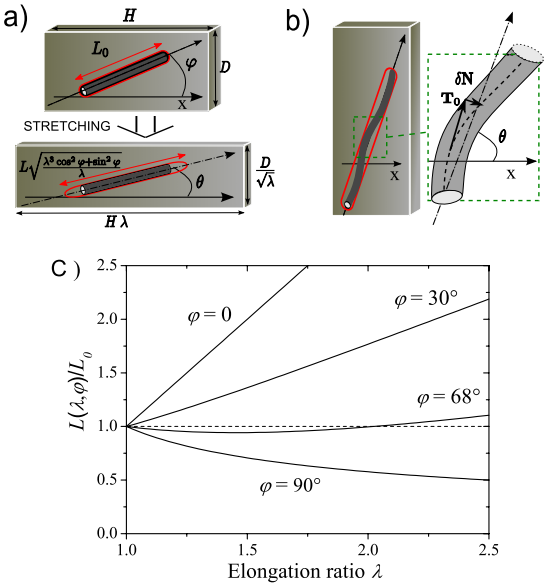

FIG. 4. (Color online) (a) Sketch of an affine deformation at constant volume of the composite under uniaxial stretching, illustrating changes in the dimensions of the sample, in the length of the polymer envelope and in the zenithal angle of the envelope with respect to the stretch axis. (b) Sketch of a buckling nanotube oriented at a large initial zenithal angle. (c) Evolution of the polymer envelope length of a tube in the frame of the affine deformation model.

During affine deformation, each PVA envelope reorients from its starting zenithal angle φ to a final zenithal angle θ [Fig. 4(a)], such that $\tan\theta=\lambda^{-3/2}\tan\varphi$, while the azimuthal angle (which describes the orientation of the projection of the nanotube on the plane perpendicular to the stretching axis) remains constant. The envelope length L_0 then changes to $L(\lambda,\varphi)=L_0(\lambda^3\cos^2\varphi+\sin^2\varphi)^{1/2}\lambda^{-1/2}$ and the uniform distribution probability $p(\varphi)=\sin\varphi$ $(0\leq\varphi\leq\pi/2)$ transforms into $p(\theta)$ such that $p(\varphi)d\varphi=p(\theta)d\theta$. The final order parameter therefore writes

$$S_g=\int_0^{\pi/2}\frac{3\cos^2\theta-1}{2}p(\theta)d\theta$$

$$=\int_0^{\pi/2}\frac{3\lambda^3(\lambda^3+\tan^2\varphi)^{-1}-1}{2}\sin\varphi d\varphi$$

$$=\frac{\sqrt{\lambda^3-1}(2\lambda^3+1)-3\lambda^3\arctan\sqrt{\lambda^3-1}}{2(\lambda^3-1)^{3/2}}, \qquad (2)$$

a simpler but equivalent equation to the expression given in Ref. 19. Globally, we find a good agreement between experiments and calculations which is in variance with the results of Ahir *et al.*[19] who found a much weaker orientation for multiwall carbon nanotubes dispersed in a semisolid rubbery polydimethylsiloxane silicon elastomer and orientated under strain. This indicates that a good dispersion of individual nanotubes is a key parameter to observe a transfer of the orientation from the matrix to the nanotubes. This point however does not explain why, for moderate strains ($\lambda<2$), the experimental order parameter is systematically larger than

the calculated value (Fig. 3). This phenomenon is hardly explained by the presence of aggregates or by a slight departure from an affine uniaxial deformation (we found experimentally that the width D of sample changes rather as $D\lambda^{-0.55}$). We therefore revisited hypotheses used in the affine deformation model. SWCNT in water have a persistence length of about one micron[31] and therefore can be considered as a straight rod *in the absence* of mechanical constraints. The affine deformation model neglects the elastic interactions between SWCNT and the matrix and implicitly considers that nanotubes oriented far from the stretching direction **x** remain straight under compression. A more realistic model consists in considering the effect of buckling, frequently encountered for nanotubes embedded in polymer matrices.[32] To check if this could explain the increase in S, we have estimated its influence on the mean orientation as a correction of the geometric model.

In the affine deformation model, the length of a polymer envelope changes as $L(\lambda,\varphi)=L_0(\lambda^3\cos^2\varphi+\sin^2\varphi)^{1/2}\lambda^{-1/2}$. Its evolution is shown in Fig. 4(c) for several initial orientations φ. It monotonically increases for tubes oriented nearly along the stretching direction but might decrease at moderate strains for orientations more perpendicular. For a given elongation ratio λ, this defines a critical initial angle $\varphi_c(\lambda)$, such that $L(\lambda,\varphi_c)=L_0$, below which only the simple geometric reorientation of the tubes is expected. Above $\varphi_c(\lambda)$ the tubes are submitted to a compression and might buckle. The fraction of such tubes becomes non-negligible at moderate strains ($\varphi_c\approx 68°$ for $\lambda=2$). The exact deformation of such buckling SWCNT in a polymer matrix is a complex problem but the resulting modification on the order parameter can be simply estimated. An upper limit of this effect is obtained by considering that the tubes get slightly and randomly curved while keeping their mean orientation in order to occupy a region of decreasing length $L(\lambda,\varphi)$. They locally deviate [see Fig. 4(b)] from their mean director $\mathbf{T}_0$ by $\delta\mathbf{N}$, where **N** is a unit vector perpendicular to $\mathbf{T}_0$. Considering only small deformations ($\delta \ll 1$), the constant tube length L_0 writes

$$L_0 = L(\lambda,\varphi) + \left\langle \int \frac{\delta^2}{2} ds \right\rangle \tag{3}$$

where s is a tube curvilinear coordinate and $\langle\ \rangle$ represents an average over the nanotubes oriented on average along $\theta > \theta_c$. Using this relation in the corrected order parameter, one gets

$$S_c = S_g + \frac{3}{2}\int_{\theta_c}^{\pi/2} \left\{ \left\langle \frac{[(\mathbf{T}_0+\delta\mathbf{N})\cdot\mathbf{x}]^2}{1+\delta^2} \right\rangle - \cos^2(\theta) \right\} p(\theta) d\theta \tag{4}$$

which, after a Taylor expansion in δ and straightforward computations, yields

$$S_c \approx S_g + \frac{3}{2}\int_{\varphi_c}^{\pi/2} \frac{\tan^2\varphi - 2\lambda^3}{\lambda^3+\tan^2\varphi}\left(1-\frac{L(\lambda,\varphi)}{L_0}\right)\sin\varphi d\varphi. \tag{5}$$

The corrected order parameter (dashed line in Fig. 3) is found to be closer to the experimental points. This model should provide a better description of the reorientation of individual SWCNT in a polymer matrix.

In summary, we showed that SWCNT can be dispersed homogeneously and individually in a PVA matrix by using a DNA wrapping. Polarized Raman and PL spectroscopies were used to describe the orientational order of nanotubes aligned in the composite by uniaxial hot stretching. The hypothesis that only a single component, namely, the zz one of the Raman polarizability tensor is nonzero is validated by the measurements: (i) the spectra are strongly polarized, with a *HH* spectrum which vanishes when the order parameter increases, (ii) for each sample, spectra measured in different polarization configurations display similar profiles and superimpose all over the spectral range after a simple normalization. Finally a good agreement is found with a simple geometrical model considering only stretching-induced reorientations of the nanotubes in PVA envelopes and a correction due to the buckling of compressed tubes.

This work was supported by the ANR P-NANO program NATALI and by a France Venezuela Post-graduate Cooperation Program (PCP). C.Z.-L. acknowledges Fundayacucho-Venezuela/CROUS-France scholarship.

*eric.anglaret@lcvn.univ-montp2.fr

[1] T. K. Leeuw *et al.*, Nano Lett. **8**, 826 (2008).
[2] J. A. Fagan *et al.*, J. Phys. Chem. B **110**, 23801 (2006).
[3] Z. Wang *et al.*, Nanotechnology **18**, 455709 (2007).
[4] B. Vigolo *et al.*, Science **290**, 1331 (2000).
[5] A. B. Dalton *et al.*, Nature (London) **423**, 703 (2003).
[6] P. Miaudet *et al.*, Nano Lett. **5**, 2212 (2005).
[7] M. Maugey *et al.*, J. Nanosci. Nanotechnol. **7**, 2633 (2007).
[8] Y. Kim *et al.*, Appl. Phys. Lett. **86**, 073103 (2005).
[9] S. Kazaoui *et al.*, Appl. Phys. Lett. **87**, 211914 (2005).
[10] V. Scardaci *et al.*, Physica E **37**, 115 (2007).
[11] S. Bachilo *et al.*, Science **298**, 2361 (2002).
[12] W. Li *et al.*, Bull. Mater. Sci. **29**, 313 (2006).
[13] P. G. De Gennes and J. Prost, *The Physics of Liquid Crystals* (Oxford University Press, New York, 1993).
[14] M. F. Islam *et al.*, Phys. Rev. Lett. **92**, 088303 (2004).
[15] J. Lagerwall *et al.*, Adv. Mater. **19**, 359 (2007).
[16] M. D. Lynch and D. L. Patrick, Nano Lett. **2**, 1197 (2002).
[17] G. Scalia *et al.*, Soft Matter **4**, 570 (2008).
[18] E. Anglaret *et al.*, Phys. Rev. B **65**, 165426 (2002).
[19] S. V. Ahir *et al.*, Phys. Rev. B **73**, 085420 (2006).
[20] S. V. Ahir *et al.*, Polymer **49**, 3841 (2008).
[21] J. A. Fagan *et al.*, Phys. Rev. Lett. **98**, 147402 (2007).
[22] G. S. Duesberg *et al.*, Phys. Rev. Lett. **85**, 5436 (2000).
[23] C. Zamora-Ledezma *et al.*, Nano Lett. **8**, 4103 (2008).
[24] P. Nikolaev *et al.*, Chem. Phys. Lett. **313**, 91 (1999).
[25] S. Badaire *et al.*, Adv. Mater. **17**, 1673 (2005).
[26] P. H. Tan *et al.*, Phys. Rev. Lett. **99**, 137402 (2007).
[27] C. Zamora-Ledezma *et al.*, Carbon **46**, 1253 (2008).
[28] M. J. O'Connell *et al.*, Science **297**, 593 (2002).
[29] C. Richard *et al.*, Science **300**, 775 (2003).
[30] H. H. Gommans *et al.*, J. Appl. Phys. **88**, 2509 (2000).
[31] R. Duggal and M. Pasquali, Phys. Rev. Lett. **96**, 246104 (2006).
[32] O. Lourie *et al.*, Phys. Rev. Lett. **81**, 1638 (1998).